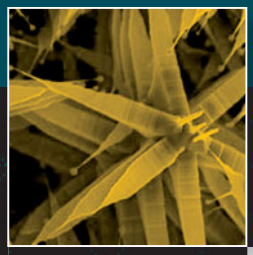

From nanogenerators to piezotronics—A decade-long study of ZnO nanostructures

Zhong Lin Wang

The following article is based on the MRS Medal Lecture, presented by Zhong Lin Wang on November 30, 2011, at the 2011 Materials Research Society Fall Meeting in Boston. The MRS Medal is awarded for a specific outstanding recent discovery or advancement that has a major impact on the progress of a materials-related field. Wang received the award for "seminal contributions in the discovery, controlled synthesis, and fundamental understanding of ZnO nanowires and nanobelts, and the design and fabrication of novel, nanowire-based nanosensors, piezotronic devices, and nanogenerators."

Developing wireless nanodevices and nanosystems is critical for sensing, medical science, environmental/infrastructure monitoring, defense technology, and even personal electronics. It is highly desirable for wireless devices to be self-powered without using a battery. We have developed piezoelectric nanogenerators that can serve as self-sufficient power sources for micro-/nanosystems. For wurtzite structures that have non-central symmetry, such as ZnO, GaN, and InN, a piezoelectric potential (piezopotential) is created by applying a strain. The nanogenerator uses the piezopotential as the driving force, responding to dynamic straining of piezoelectric nanowires. A gentle strain can produce an output voltage of up to 20–40 V from an integrated nanogenerator. Furthermore, piezopotential in the wurtzite structure can serve as a "gate" voltage that can effectively tune/control charge transport across an interface/junction; electronics based on such a mechanism are referred to as piezotronics, with applications such as electronic devices that are triggered or controlled by force or pressure, sensors, logic units, and memory. By using the piezotronic effect, we show that optoelectronic devices fabricated using wurtzite materials can provide superior performance for solar cells, photon detectors, and light-emitting diodes. Piezotronic devices are likely to serve as "mediators" for directly interfacing biomechanical action with silicon-based technology. This article reviews our study of ZnO nanostructures over the last 12 years, with a focus on nanogenerators and piezotronics.

Introduction

ZnO is one of most the important materials in materials research today. ZnO nanowires have attracted worldwide attention because of important implications in LED, biomedical, solar cell, and electronics applications. Our research has focused on this material, but we have ventured beyond building nanostructures to building self-powered nanosystems. Our research on ZnO started in 1999 and continues today.[1] From a structural point of view, ZnO has a non-central symmetric wurtzite crystal structure, which naturally produces a piezoelectric effect once the material is strained. Zn^{2+} cations and O^{2-} anions are tetrahedrally coordinated, and the centers of the positive and negative ions overlap. If a stress is applied at an apex of the tetrahedron, the centers of the cations and anions are relatively displaced, resulting in a dipole moment (**Figure 1**a). Polarization from all of the units results in a macroscopic potential (piezopotential) drop along the straining direction in the crystal (Figure 1b).[2] By using this potential generated inside the crystal as an acting/controlling field, two new fields are created. Piezopotential-driven transient flow of electrons in an external load is the principle of the nanogenerator (NG);[3–5] piezopotential tuned/controlled charge transport inside the crystal is the principle behind piezotronics.[6,7]

Zhong Lin Wang, School of Materials Science and Engineering, Georgia Institute of Technology; zhong.wang@mse.gatech.edu
DOI: 10.1557/mrs.2012.186

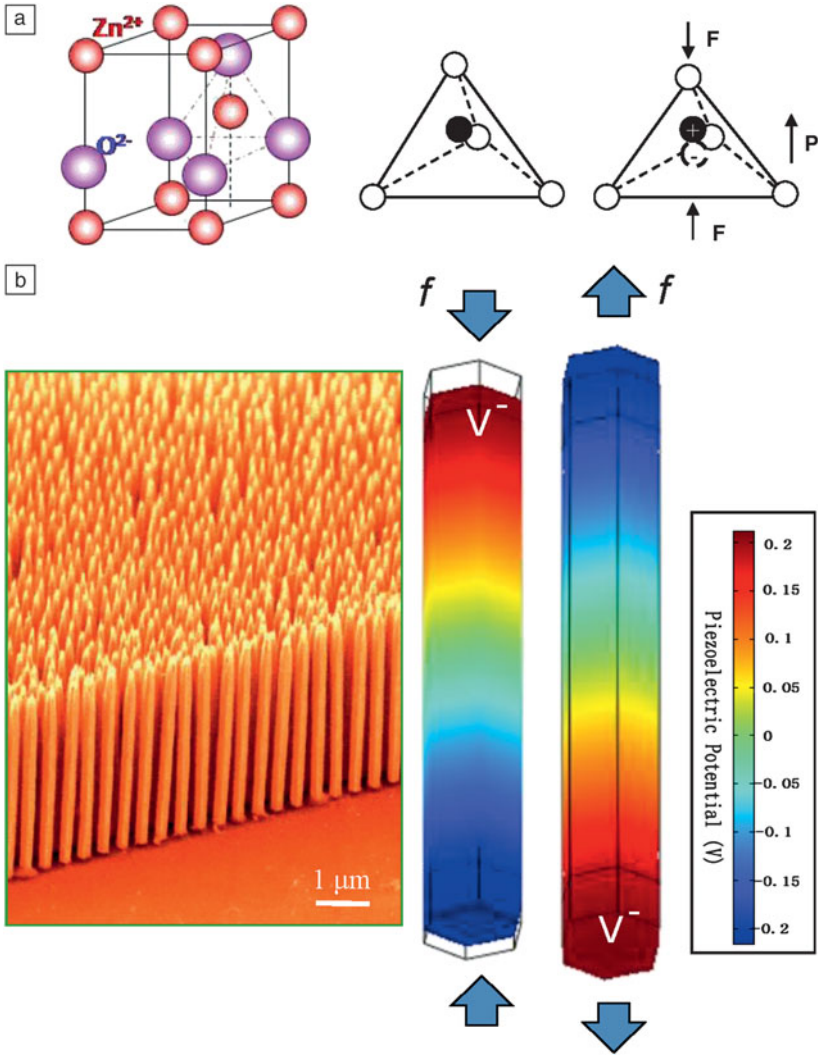

Figure 1. Piezopotential in a wurtzite crystal. (a) Atomic model of the wurtzite-structured ZnO. (b) Scanning electron microscopy image of aligned ZnO nanowire (NW) arrays synthesized using a solution-based approach (left image). Numerically calculated distribution of piezoelectric potential along a ZnO NW under axial strain: compressive strain (middle image) and tensile strain (right image). The growth direction of the NW is the *c*-axis. The dimensions of the NW are L = 600 nm and a = 25 nm; the external force is f_y = 80 nN.

Growth of unique nanostructures

The discovery of nanobelts, ultralong ribbon-like nanostructures, in 2001 was the start of our research in oxide nanostructures.[8] Since then, we have focused mainly on ZnO, which has the most splendid nanostructure configurations among all known materials.[9,10] The wurtzite structure of ZnO is unique for its non-central symmetry and polar surfaces. The structure of ZnO can be described as a number of alternating planes composed of tetrahedrally coordinated O^{2-} and Zn^{2+} ions, stacked alternatively along the *c*-axis. The oppositely charged ions produce positively charged (0001)-Zn and negatively charged $(000\bar{1})$-O polar surfaces, resulting in a normal dipole moment and spontaneous polarization along the *c*-axis as well as a divergence in surface energy. The electrostatic interaction energy and distinct chemical activities of the polar surfaces result in the formation of a wide range of nanostructures, such as nanosprings,[11] nanorings,[12] nanobows,[13] and nanohelices[14] (**Figure 2**).

ZnO nanobelts and the associated unique nanostructures shown in Figure 2 were grown using a vapor-solid process without a metal catalyst.[8] For a nanobelt dominated by the polarized ±(0001) facets, a spontaneous polarization is induced across the nanobelt thickness due to the positive and negative ionic charges on the zinc- and oxygen-terminated ±(0001) surfaces, respectively. As a result, a nanospring is formed when a single-crystal nanobelt rolls up; this phenomenon is attributed to a consequence of minimizing the total energy contributed by spontaneous polarization and elasticity. Alternatively, a nanoring can be initiated by circular folding of a nanobelt so that the oppositely charged surfaces meet face-to-face. Coaxial and uniradial loop-by-loop winding of the nanobelt forms a complete ring. Short-range chemical bonding among the loops results in a single-crystal structure. The self-coiling is likely to be driven by minimizing the energy contributed by polar charges, surface area, and elastic deformation.[8]

Vertically aligned ZnO nanowire (NW) arrays are probably the most important structure for applications, such as solar cells,[15] field emission devices,[16] UV lasers,[17] light-emitting diodes,[18] and piezo-nanogenerators.[2,19,20] Aligned growth of ZnO nanorods has been successfully achieved on a solid substrate using a vapor-liquid-solid or vapor-solid-solid process using gold nanoparticles as catalysts,[13,21] where the catalyst initiates and guides growth, and the epitaxial orientation relationship between the nanorods and the substrate leads to aligned growth.[22] The spatial distribution of the catalyst particles determines the pattern of the grown NWs. By choosing an optimum match between the substrate lattice and the desired NWs, epitaxial orientation between the NW and substrate results in aligned growth of NWs normal to the substrate. The distribution of the catalyst particles defines the locations of the NWs, and the epitaxial growth on the substrate results in vertical alignment.

Solution based growth of ZnO is one of the most powerful low-cost, low-temperature, and large-scale approaches for aligned NWs.[23–25] The growth temperature is around 80–100°C, so the substrate can be any material with any shape. This allows a broad range of applications.

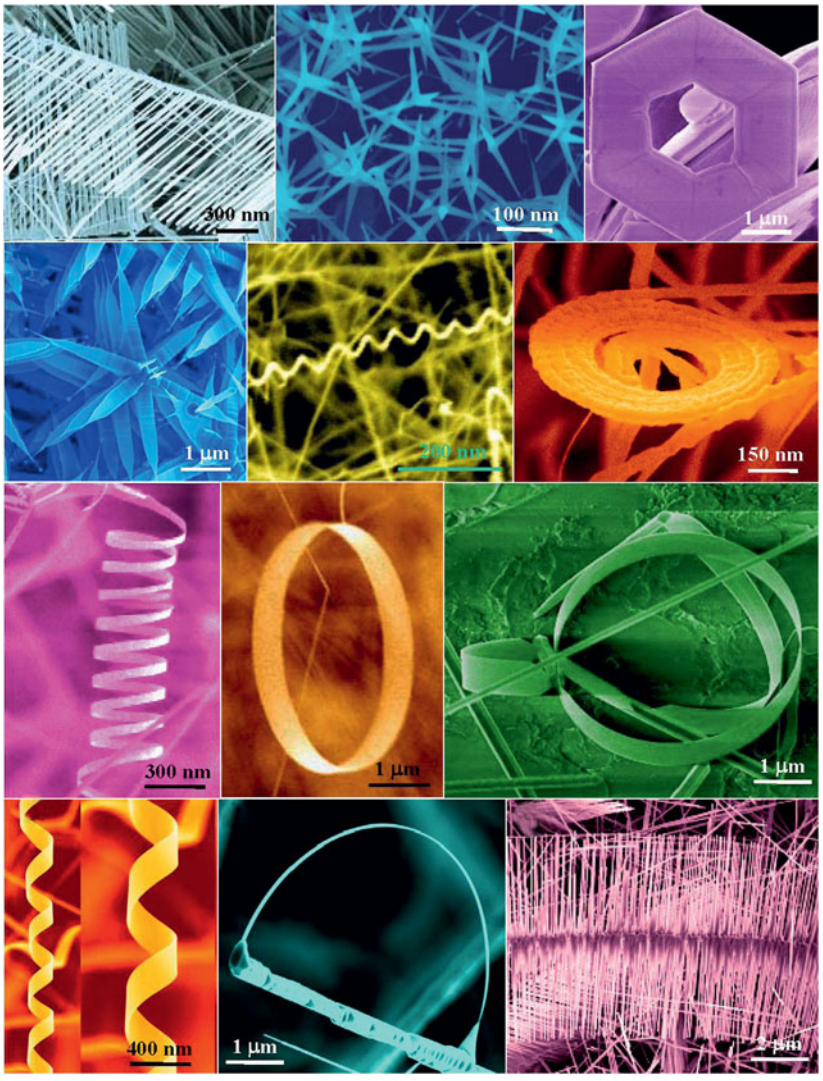

Figure 2. A collection of novel ZnO nanostructures that were formed due to the existence of ±(0001) polar surfaces.[1]

Nanogenerators

Lateral nanowire based nanogenerators

In today's micro-/nanoscale devices, power consumption is small. Medical sensing, remote patient monitoring, environmental monitoring, long-range asset tracking, and national security all require a large number and high density of sensors. In this case, we would like sensors to be self-powered, and the device could simply generate its own power from the environment. This is called "self-powered nanotechnology."[26] For this, we tried to utilize the functionality of ZnO. The goal of our research is to use our daily activity as small-scale mechanical action. In order to do this, we rely on the piezoelectric effect. One of the unique advantages of ZnO is that all of the NWs grow along the *c*-axis (i.e., in the polar direction) and are uniaxially aligned. Once the NWs are strained, a macroscopic piezopotential is created, which can drive a flow of electrons, thus converting mechanical energy into electricity. We started this work in 2005, using conducting atomic force microscopy to deform a single NW.[1] We have developed nanogenerators (NGs) that can give an output of 50 V at an ideal peak power density of ~0.5 W/cm^3.[27]

A single NW laterally bonded on a flexible substrate can be used to illustrate the principle of NG (**Figure 3**a).[28] A Schottky contact on at least one side of the contact is required for a functioning NG. The entire wire is in an equilibrium state without strain and power output (Figure 3b). When the wire is stretched, the piezopotential created results in a difference in the Fermi levels of the two contacts at the ends of the wire (Figure 3c). The electrons in the external circuit flow from the right-hand side to the left-hand side to compensate for the energy difference. The electrons cannot flow across the interface due to the presence of a Schottky barrier ϕ_{SB}. The accumulation of the electrons at the interface partially screen the piezopotential built in the wire. When the electrons and the piezoelectric field reach equilibrium, the Fermi energy on both sides is equal, and there is no more current flow (Figure 3d). When the single wire generator (SWG) is quickly released, the polarization and piezoelectric field vanish, and the equilibrium with the accumulated electrons is broken. The accumulated charge carriers flow back from the left-hand side to the right-hand side through the external circuit, producing the second output signal in the opposite direction (Figure 3e). The energy band diagrams (Figure 3b–e) show the generation of a pair of positive and negative voltage/current peaks with a polarity as assumed for the case. This is the process of the experimentally observed ac output (Figure 3f). When the wire is cyclically "fast stretched" (FS) and "fast released" (FR), output electricity is obtained.

Integration of SWGs is a major step toward practical applications. We can transfer millions of NWs onto a single substrate for improving the output.[29] For the structure shown in **Figure 4**, the output voltage reached 2 V, and the current reached 100 nA.

Vertical nanowire based nanogenerators

Using the as-grown, well-aligned NWs, high output NGs have been fabricated. **Figure 5**a shows a new approach we developed recently for fabricating a high-output, low-cost NG.[30] The entire structure is based on a polystyrene (PS) substrate of typical thickness 0.5 mm, on which a Cr adhesion layer is deposited. After sputtering a layer of ZnO seed, densely packed ZnO NWs are grown on the seed layer as a quasi-continuous "film" using a solution based growth technique at a temperature no more than 100°C. Finally, a thin layer of poly(methyl

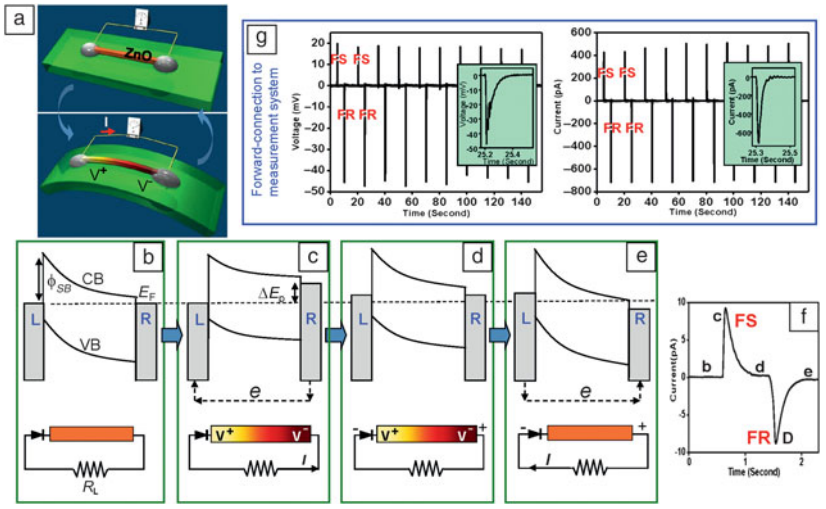

Figure 3. Charge generation and output mechanism of an alternating-current single wire nanogenerator illustrated using an energy band diagram. (a) Schematic of a ZnO wire contacted with two metal electrodes, at equilibrium (upper) and stretched (lower). Energy band diagrams of the device when the wire is at equilibrium (b), tensile stretched (c), returns to equilibrium (d), and then released (e). In the lower portion of each is a sketch of the measurement circuit, where a small load resistor R_L is introduced, which is much smaller than the resistance of the wire and/or the contacts. (f) An experimentally measured output current from the nanogenerator, in which the output regions corresponding to the processes shown in (b–e) are indicated by the corresponding labels (b–e). (g) Experimentally measured output voltage and current from the nanogenerator by repeated deformation.[32] FS, fast stretched; FR, fast released; VB, valence band; CB, conduction band.

methacrylate) (PMMA) was deposited on top of the film to serve as an isolation layer, followed by deposition of a thin gold layer as an electrode. The growth of ZnO NWs has a unique and distinguishing feature in that they are aligned along the *c*-axis, so that the entire film has a common polar direction. Once the PS substrate is mechanically bent/deformed through the substrate, the film at the top surface is under tensile strain, and the one at the bottom surface is under compressive strain, resulting in a piezopotential difference between the top and bottom electrodes, which drives the flow of electrons in the external load. A cycling mechanical deformation results in the back-and-forth flow of electrons in response to the mechanical triggering. By introducing a strain of 0.12% at a strain rate of 3.56 % S^{-1}, the measured output voltage reached ~20 V, and the output current exceeded 8 μA (corresponding to an ideal maximum power density of 0.16 W/cm^3) (Figure 5b–c).[30] The total output can be enhanced by integrating multiple NGs in series or parallel depending on the application so that the entire system can be placed, for example, in shoes, clothes, plastic sheets, and rotating tires. The advantage of using NWs is that they can be triggered by tiny physical motions, and the excitation frequency can be one Hz to thousands of Hz, which is ideal for harvesting random energy in the environment such as tiny vibrations, body motion, and gentle air flow.

In some cases, alignment of the NWs is not essential for generating electricity. Using the conical shape of the ZnO NWs, a ZnO–polymer composite can also be used to generate electricity.[31] Such an idea can be extended to a general composite between a polymer and NWs, such as $NaNbO_3$.[32] Applying a polarization perpendicular to the composite film can produce a macroscopic piezopotential in the film, which then generates electricity.

Self-powered nanosystems

A nanosystem is an integration of multifunctional nanodevices. The power required to drive such electronics is in the microwatt to milliwatt range. It is possible to have self-powered, maintenance-free biosensors, environmental sensors, nanorobotics, microelectromechanical systems (MEMS), and even portable/wearable electronics.[33] An NG was fabricated using aligned NW arrays (To view supplementary material for this article, please visit http://dx.doi.org/10.1557/mrs.2012.186.), which powered a pH sensor made of a single NW. To demonstrate the operation of an NG driven self-powered system (**Figure 6**a), we used a single transistor radio frequency (RF) transmitter to send out a detected electric signal.[34,35] The oscillation frequency

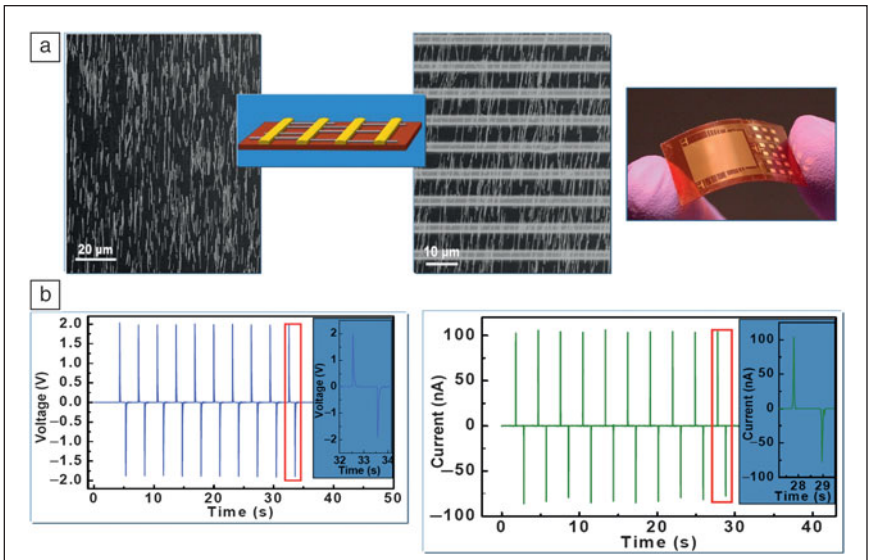

Figure 4. (a) High output nanogenerator (NG) obtained by using the integration of millions of nanowires transferred to a polymer substrate following the approach presented in Figure 3a. Scanning electron microscopy images before (far left) and after (right) depositing Au electrodes and corresponding schematic and real NG device (far right). (b) The packaged NG gives an output voltage of 2 V (left) and current of 100 nA (right). The insets are enlarged signals from one cycle of deformation taken from the areas inside the red rectangles.[33]

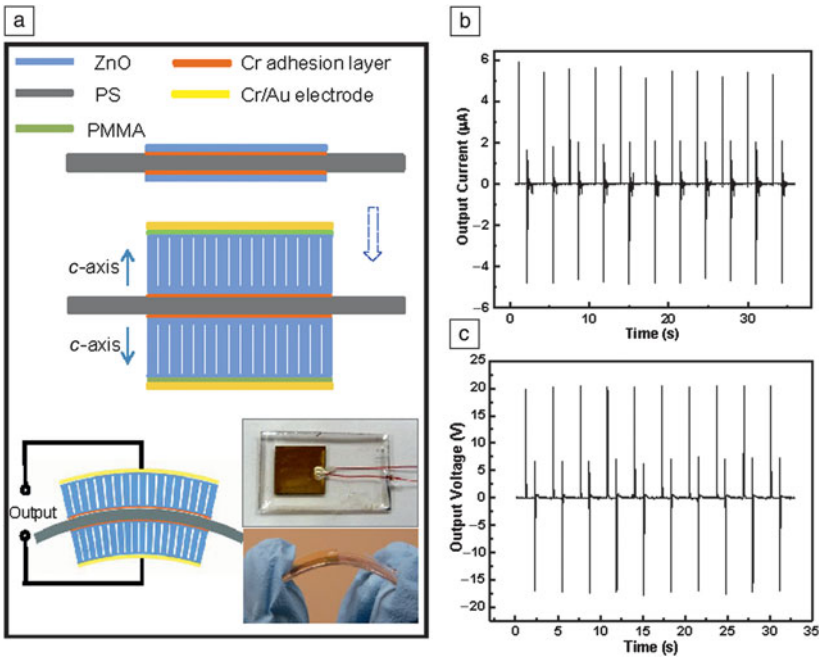

Figure 5. Fabrication of a high output nanogenerator using vertically aligned nanowire arrays/films grown on two sides of a polymer film. (a) Fabrication process of the nanogenerator. The lower right part is a photo of a fabricated nanogenerator after packaging. The bending of the nanogenerator shows good mechanical flexibility. (b) Output current and (c) output voltage of a typical nanogenerator.[31]

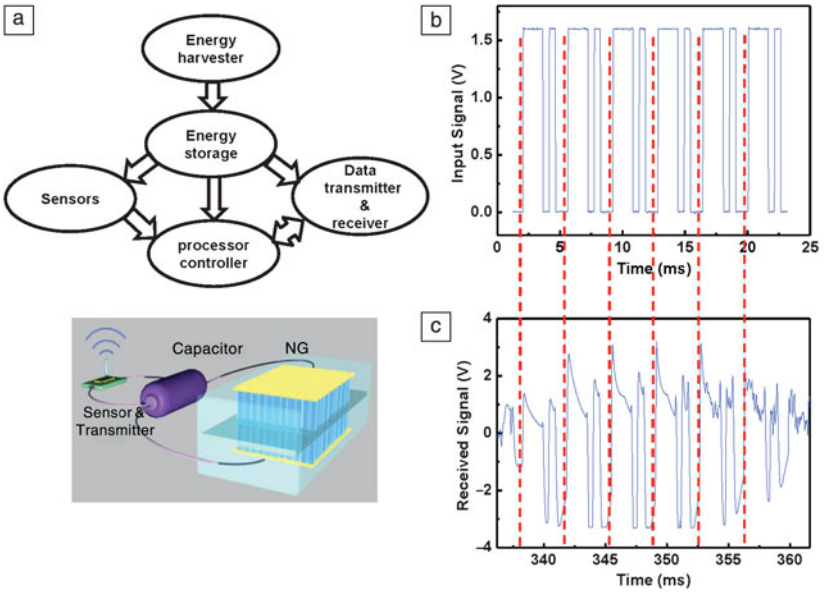

Figure 6. (a) Schematic diagram of an integrated self-powered system that can be divided into five modules: energy harvester, energy storage, sensors, data processor and controller, and data transmitter and receiver. (b) The voltage sequence used to trigger the sensor, representing a waveform envelope of the input signal. (c) Recorded signal from the headphone jack of the radio located 10 m away, showing the technical feasibility of a wireless self-powered system.[34,35]

was tuned to be around 90 MHz, and a commercial portable AM/FM radio was used to receive the transmitted signal. The entire system is made of the NG, a capacitor for energy storage (to regulate output power), the sensor signal modulator, and the wireless rf data transmitter. For demonstrating the synchronization between the sensed signal and the signal transmitted, a phototransistor in a slotted optical switch was added to the system as the photon detecting sensor to demonstrate that the self-powered system can work independently and wirelessly. The signal of the photocurrent generated by the phototransistor as a result of external light excitation was periodically sent out using the energy stored in the capacitor. Each time it was triggered, the signal received by the phototransistor modulated the transmitting signal, and the information was received by the radio, and the demodulated signal was recorded from the headphone jack. Each cycle included an on (16 ms)/off (5 ms)/on (5 ms)/off (10 ms) status sequence. Figure 6b is the signal demodulated by the radio. When the phototransistor and the transmitter were triggered, there was a pulse detected beyond the noise background. When we enlarged this pulse, it contained a segment of the information that had the same waveform envelope as the triggering voltage sequence of the LED, as shown in Figure 6c. This indicates that the wireless data transmission was achieved by using this self-powered system over a distance of ~10 m.[34,35]

Hybrid cell for simultaneously harvesting multiple types of energies

Our environment has an abundance of energy forms, including light, thermal, mechanical (such as vibration, sonic waves, wind), magnetic, chemical, and biological. Harvesting these types of energies is of critical importance for long-term energy needs and sustainable development. Innovative approaches have to be developed for conjunctional harvesting of multiple types of energies using an integrated structure/material so that the energy resources can be effectively and complimentarily utilized whenever and wherever one or all of them are available. We initiated an idea in 2009 for harvesting multiple types of energy using a single device structure, known as a hybrid cell (HC) (**Figure 7**a).[36] The structure is based on vertical ZnO NW arrays but with the addition of a solid electrolyte and a metal coating.[37] The solar cell open circuit voltage ($U_{OC\text{-}SC}$) was

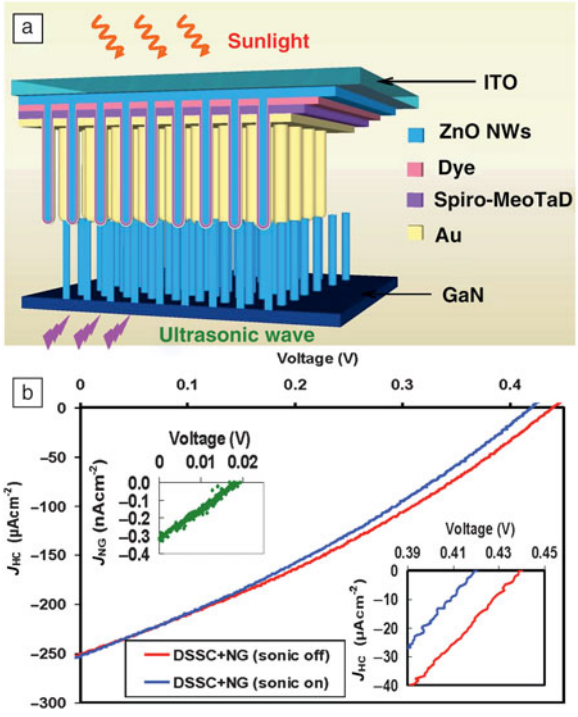

Figure 7. Design of a compact hybrid cell (HC) structure consisting of a dye sensitized solar cell (DSSC) and a nanogenerator (NG). (a) Schematic illustration of the HC, illuminated by sunlight from the top and excited by ultrasonic waves from the bottom. The ITO layer on the DSSC and the GaN substrate are defined as the HC cathode and anode, respectively; Spiro-MeoTaD is a polymer. (b) A comparison of power output *J–V* characteristics of a HC. The top left inset is the *I–V* characteristic of the NG when the solar cell is off. The bottom right inset is a replot of the displayed curves at short circuit.[37]

0.42 V, and the short circuit current density ($J_{SC\text{-}SC}$) was 0.25 mA cm^{-2}. The NG was characterized by introducing ultrasonic waves through a water medium without sunlight illumination; the corresponding *J–V* curve shows that $U_{OC\text{-}NG}$ was ~0.019 V, and I_{NG} was ~0.3 pA cm^{-2}. When only simulated sunlight shines on the HC, the dye-sensitized solar cell (DSSC) worked (Figure 7b), and the optimum output power density was found to be 32.5 μWcm^{-2} at J_{SC} = 140 μAcm^{-2} and U_{OC} = 0.231 V. When both the DSSC and NG were simultaneously operating in series, the corresponding output power density was 34.5 μWcm^{-2} at J_{SC} = 141 μAcm^{-2} and U_{OC} = 0.243 V. After the ultrasonic wave was turned on, power density increased (ΔP_{HC}) by 2 μWcm^{-2}, which represented more than a 6% enhancement in optimum power output. Therefore, in addition to enhancing the open circuit voltage, the HC successfully added the total optimum power outputs from both the solar cell and the NG.

With the development of modern medical technology, powering implantable nanodevices for biosensing using energy harvesting technology has become a challenge. We developed a HC for harvesting mechanical and biochemical energies[38] mainly for biomedical applications. The structure is based on an integrated NW-based NG system and an enzyme-based biofuel cell (BFC). In this hybridized design, we used piezoelectric poly(vinylidene fluoride) (PVDF) nanofibers (NFs) as the working component for mechanical energy harvesting. The working principle of the PVDF NG is based on the piezoelectric properties of the PVDF NF. As the device is deformed under alternating compressive and tensile force, the NFs drive a flow of electrons back and forth through the external circuit.[17] The enzymatic BFC was used to convert the chemical energy of glucose and oxygen in the biofluid into electricity. The electrodes were patterned onto a Kapton film and coated with multiwalled carbon nanotubes, and finally immobilized glucose oxidase (GOx) and laccase form the anode and cathode, respectively, for the BFC. A HC structure can be fabricated on a single PVDF NF for energy harvesting.[39]

Nanogenerators as active sensors

A nanogenerator can also function as an active sensor by using its electric output as the signal to be detected. Based on such an idea, we recently demonstrated a self-powered sensor for detecting low frequency vibrations.[40] Furthermore, we fabricated a self-powered pressure sensor based on the BFC and NG on a single fiber,[41] as shown in **Figure 8**a. ZnO NW films grown around a carbon fiber forms a textured film with the *c*-axis radially pointing outward. Mechanical straining would generate a piezopotential across the thickness of the NW film (Figure 8b). Thus, the output of the NG is sensitive to the pressure change. This experiment demonstrates that not only can we use the HC or NG as an energy harvester, but also as an active sensor for detecting a mechanical signal from the environment.

Piezotronics

In order to illustrate the basic concept of piezotronics, we first start from a traditional metal oxide semiconductor field-effect transistor (MOSFET). For an *n*-channel MOSFET (**Figure 9**a), the two *n*-type doped regions are the drain and source; a thin insulator oxide layer is deposited on the *p*-type region to serve as the gate oxide, on which a metal contact is made as the gate. The current flowing from the drain to the source under an applied external voltage V_{DS} is controlled by the gate voltage V_G, which controls the channel width for transporting the charge carriers. A piezotronic transistor is a metal-NW-metal structure, as schematically shown in Figure 9b once a strain is applied through the substrate.[41] The fundamental principle of the piezotronic transistor is to control the carrier transport at the metal-semiconductor interface through tuning at the local contact by creating a piezopotential at the interface region in the semiconductor by applying a strain. This structure is different from the complementary metal oxide semiconductor (CMOS) design. First, the externally applied gate voltage is replaced by an inner crystal potential generated by the piezoelectric effect, thus, the "gate" electrode is eliminated. This means that the piezotronic transistor only has two leads: drain and source. Second, control over channel width is replaced by control at the interface. Since

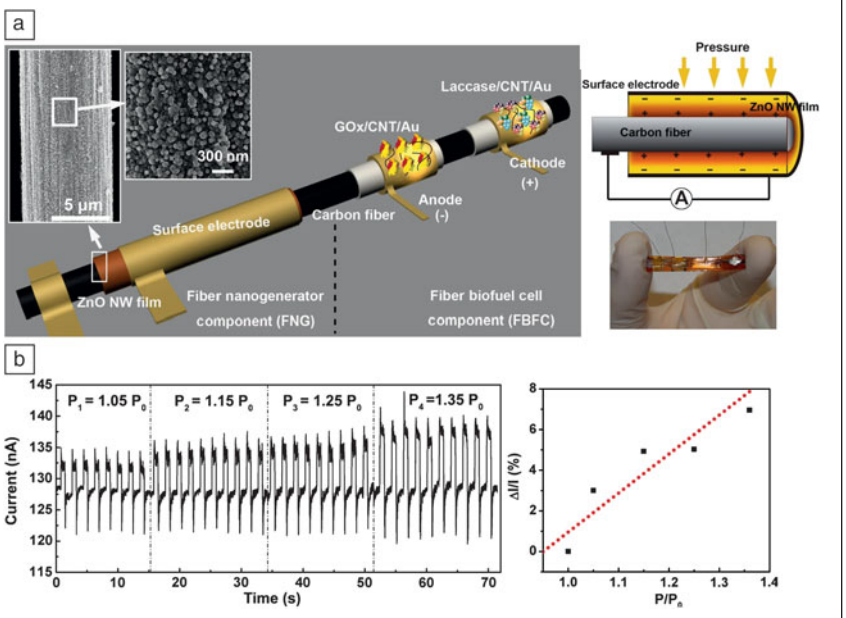

Figure 8. Integration of a nanogenerator and a biofuel cell along a single fiber as a hybrid cell or a self-powered pressure sensor. (a) Schematic diagram of the design. Inset scanning electron microscopy images show the ZnO nanowire film. The right-hand side shows the principle of the fiber-based nanogenerator (top) along with a photograph of the as-fabricated device (bottom). (b) Pressure measurement in a bio-liquid using a hybrid nanogenerator as a self-powered system. The response of the hybrid nanogenerator system to periodically applied pressure is shown on the left. Plot of the statistically measured steady current from left as a function of applied pressure, showing a linear relationship, is on the right.[41]

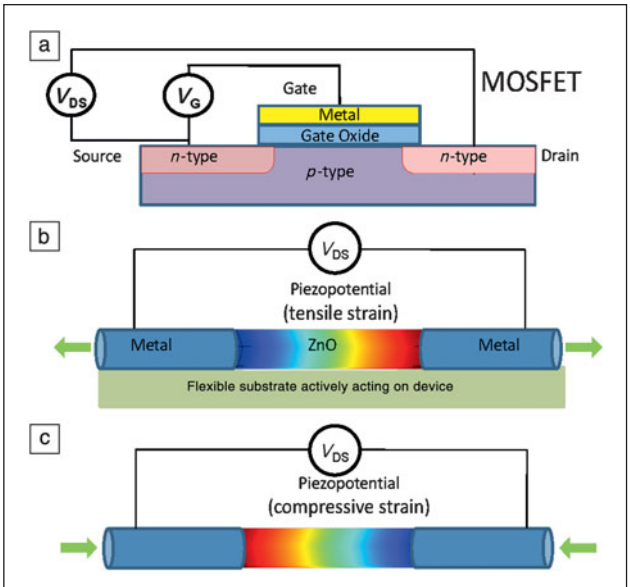

Figure 9. Schematic of (a) an *n*-channel MOSFET and (b) a semiconductor nanowire field-effect transistor. Schematic of a piezotronic transistor with tensile strain (b) and compressive strain (c), where the gate voltage that controls the channel width is replaced by a piezopotential that controls the transport across the metal-semiconductor interface. The colors represent the distribution of piezoelectric potential inside the nanowire: red is positive potential, and blue is negative potential.[41]

the current transported across an M-S interface is the exponential of the local barrier height in the reversely biased case, the ON and OFF ratio can be rather high due to the non-linear effect. Finally, a voltage controlled device is replaced by an external strain/stress controlled device, which is likely to have applications complementary to CMOS devices. The initial idea of piezotronics was first described in 2006[42] and 2007.[43,44]

When a ZnO NW device is under strain, there are two typical effects that may affect the carrier transport process. One is the piezoresistance effect[45,46] due to changes in band gap, charge carrier density and possibly density of states in the conduction band of the semiconductor crystal under strain. This effect is a symmetric effect on the two end contacts and has no polarity, which will not produce the function of a transistor. The other is the piezotronic effect due to the polarization of ions in a crystal that has non-central symmetry; this has an asymmetric or non-symmetric effect on the local contacts at the source and drain owing to the polarity of the piezopotential. In general, the negative piezopotential side raises the barrier height at the local contact of a metal/*n*-type semiconductor, possibly changing an Ohmic contact to a Schottky contact, or a Schottky contact to an "insulator" contact; while the positive piezopotential side lowers the local barrier height, changing a Schottky contact to an Ohmic contact. But the degree of change in the barrier height depends on the doping type and doping density in the NW. The piezoelectric charges are located at the ends of the wire, thus they directly affect the local contacts. The piezotronic effect is a common phenomenon for the wurtzite family, such as ZnO, GaN, CdS, and InN. It is important to point out that the polarity of the piezopotential can be switched by changing tensile strain to compressive strain (Figure 9c). Thus, the device can be changed from control at source to control at drain simply by reversing the sign of the strain applied to the device.

Piezotronic effect on metal-semiconductor contact

When a metal and an *n*-type semiconductor form a contact, a Schottky barrier (SB) ($e\phi_{SB}$) is created at the interface if the work function of the metal is appreciably larger than the electron affinity of the semiconductor (**Figure 10**a). If the semiconductor also exhibits the piezoelectric effect, a strain in the structure would produce piezo-charges at the interfacial region. It is important to note that the polarization charges are distributed within a small depth from the surface, and they are ionic charges, which are non-mobile charges located adjacent to the interface. In such a case, free carriers can only partially screen the piezo-charges due to the finite dielectric permittivity of the crystal and the limited doping concentration, but they cannot completely cancel the piezo-charges. The piezo-charges may

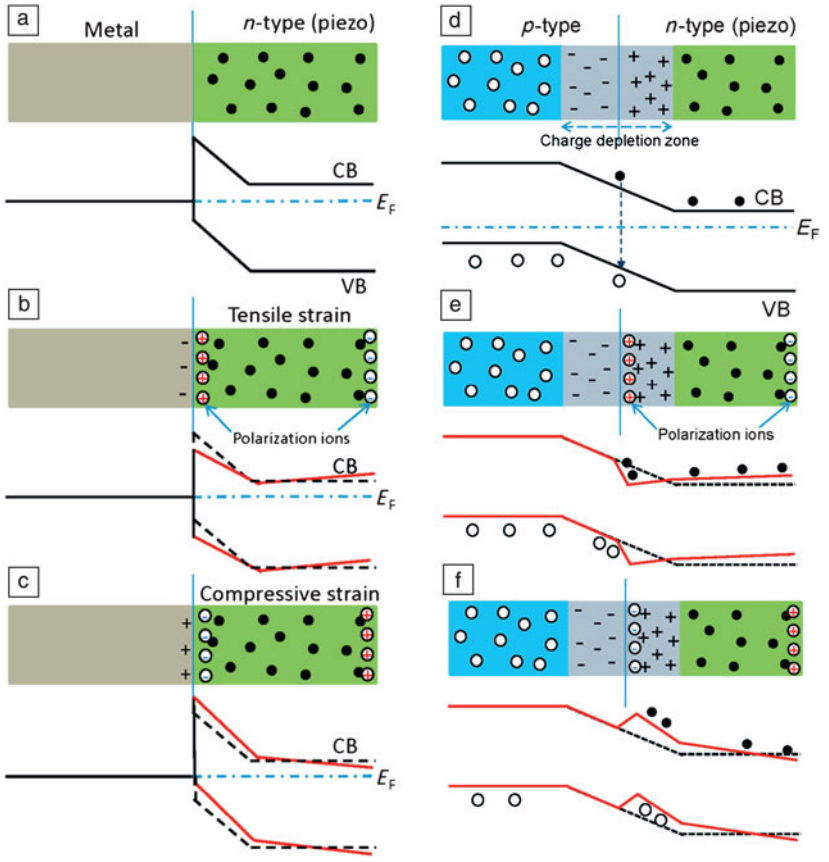

Figure 10. (a–c) Energy band diagrams illustrating the effects of piezoelectric polarization charges on a Schottky contacted metal-semiconductor interface with and without the presence of nonmobile, ionic charges at the metal-semiconductor interface. The piezoelectric charges are indicated at the interface. (d–f) Energy band diagrams illustrating the effect of piezoelectricity on a *p-n* junction made of two materials with similar bandgaps. The distorted band in the presence of piezoelectric charges is indicated by red lines.[58] VB, valence band; CB, conduction band.

produce mirror charges at the metal side. The positive piezo-charges may effectively lower the barrier height at the local Schottky contact, while the negative piezo-charges increase the barrier height (Figure 10b–c). The role played by the piezopotential is to effectively change the local contact characteristics through an internal field depending on the crystallographic orientation of the material and the sign of the strain, thus, the charge carrier transport process is tuned/gated at the M-S contact.[9,47] Therefore, the charge transport across the interface can be largely dictated by the created piezopotential, which is the gating effect. This is the core of the piezotronic effect.

Piezotronic effect on p-n *junctions*

When *p*-type and *n*-type semiconductors form a junction, the holes in the *p*-type side and the electrons in the *n*-type side tend to redistribute to balance the local potential; the interdiffusion and recombination of the electrons and holes in the junction region form a charge depletion zone. The presence of such a carrier free zone can significantly enhance the piezoelectric effect, because the piezo-charges will mostly be preserved without being screened by local residual free carriers. As shown in Figure 10d, in the case that the *n*-type side is piezoelectric and a strain is applied, local net negative piezo-charges are preserved at the junction provided the doping is relatively low such that the local free carriers do not fully screen the piezo-charges. The piezopotential tends to raise the local band slightly and introduce a slow slope to the band structure.[9] Alternatively, if the applied strain is switched in sign (Figure 10e), the positive piezo-charges at the interface creates a dip in the local band. A modification in the local band may be effective for trapping the holes so that the electron-hole recombination rate may be largely enhanced, which is very beneficial for improving the efficiency of an LED.[48] Furthermore, the inclined band tends to change the mobility of the carriers moving toward the junction.

Piezotronic transistor

A piezotronic transistor is made of a single ZnO NW with its two ends, the source and drain electrodes, fixed by silver paste on a polymer substrate (**Figure 11**a). Once the substrate is bent, a tensile/compressive strain is created in the NW, since the mechanical behavior of the entire structure is determined by the substrate. Utilizing the piezopotential created inside the NW, the gate input for a NW strain-gated transistor (SGT) is an externally applied strain rather than an electrical signal.[49] I_{DS}-V_{DS} characteristics for each ZnO-NW SGT are obtained as a function of the strain created in the SGT (Figure 11b). Positive/negative strain is created when the NW is stretched/compressed. The SGT behaves similarly to an *n*-channel enhancement-mode MOSFET, apparently indicating the working principle of the SGT.

The working principle of a piezotronic transistor is illustrated by the band structure of the device.[33] A strain free ZnO NW may have Schottky contacts at the two ends with the source and drain electrodes (Figure 11c). A piezopotential drop from V^+ to V^- is created along the NW once it is subjected to mechanical straining, which reduces and increases the local Schottky barriers (Figure 11d), respectively. This asymmetric effect on the local contacts is characteristic of the piezotronic effect. A change in the sign of strain results in a reversal of the piezopotential, thus, the polarity of the transport characteristic is changed (Figure 11e).

Based on the piezotronic transistor described previously, universal logic operations such as inverters, NAND, NOR, and XOR gates have been demonstrated for performing piezotronic logic calculations,[35] which have the potential to be integrated with MEMS technology for achieving advanced and complex functional actions. This is an outstanding example

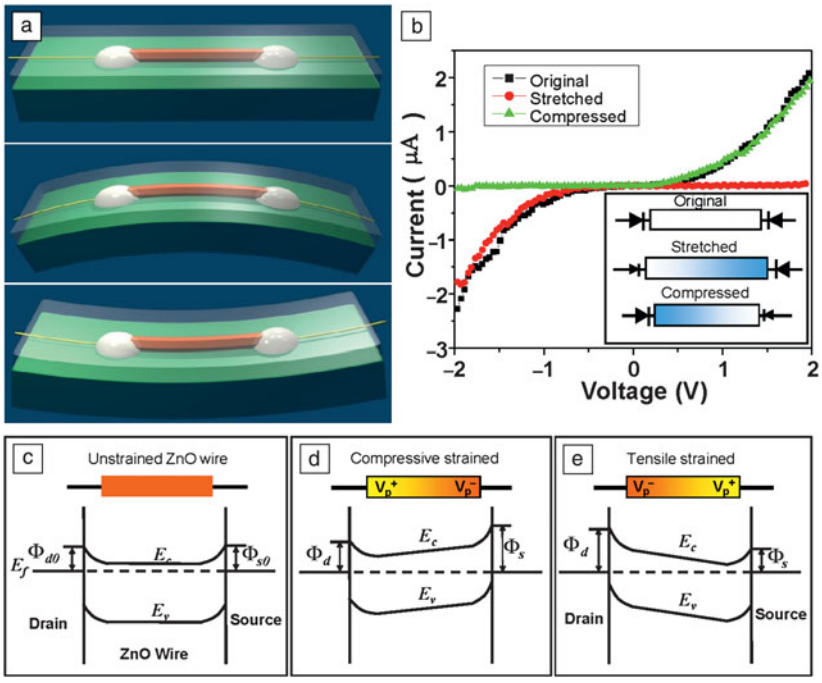

Figure 11. Piezotronic transistor. (a) Schematic of an Ag-ZnO-Ag strain gated transistor on a flexible substrate. The deformation in the transistor is indicated through a change in shape of the substrate. (b) Changes in transport characteristics of a Ag/ZnO-nanowire/Ag device from symmetric *I–V* characteristics (black) to asymmetric rectifying behavior when stretching (red) and compressing (green) the wire. Inset: equivalent circuit models of the device in corresponding to the observed *I–V* curves, different sizes of diode symbols are used to illustrate the asymmetric Schottky contacts at the two ends of the nanowire. (c–e) Band diagrams for illustrating the piezotronic effect on local contact of the device without and with the presence of piezopotential. The sign of the piezopotential is indicated in the nanowire.[49]

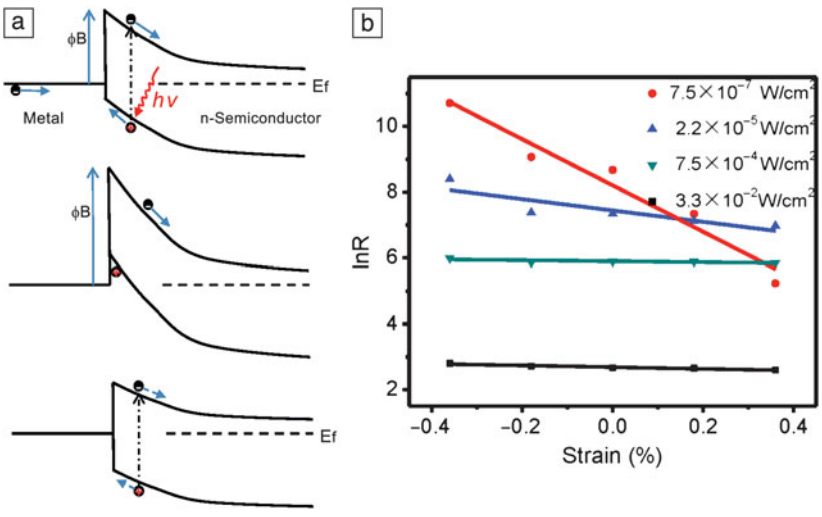

Figure 12. Enhancing photon detection sensitivity by the piezo-phototronic effect. (a) Schematic band diagrams for illustrating the effect of local piezo-charges on the Schottky contact showing the piezotronic effect on separating the photon induced charges. (b) Response of a ZnO wire UV detector (in units of A/W) as a function of strain under different excitation light intensity on a natural logarithmic scale.[55]

of using mechanical straining to generate and control digital calculation. Furthermore, using the memristor effect of ZnO, a piezoelectrically modulated resistive memory cell[50] has also been fabricated.

We have also developed the theoretical framework of piezotronics by studying charge transport across metal-semiconductor contacts and *p-n* junctions with the introduction of a piezopotential.[27] In addition to numerical calculations, we derived analytical solutions under simplified conditions and found that for an M-S contact, the current to be transported can be tuned or controlled by not only the magnitude of the strain, but also by the sign of the strain (tensile versus compressive).

Traditionally, a transistor is a device that uses an external voltage to control transport current, and it can be utilized to magnify the input electrical signal. In other words, such a device uses an electrical signal to tune/control another electrical signal. In the case of the piezotronic transistor, we use strain to control electrical signal rather than amplifying it.

Piezo-phototronics

If photon excitation is applied at a M-S contact, the newly generated electrons in the conduction band tend to move away from the contact, while the holes tend to move close to the interface toward the metal. The accumulated holes at the interface modify the local potential profile so that the effective height of the Schottky barrier is lowered (**Figure 12**a), which then increases the conductance.

On the other hand, the presence of negative piezo-charges as a result of applying strain can effectively reduce the conductance, which is a result of raising the Schottky barrier height (SBH). Therefore, laser excitation and the piezoelectric effect can be applied together for controlling charge transport at the interface. This coupling between piezoelectricity and photon excitation[51] is the piezo-phototronic effect, which uses the piezopotential for effectively controlling carrier generation, separation, transport, and/or recombination in optoelectronic processes.[9,10] We now use three examples to illustrate the piezo-phototronic effect in a photodetector, solar cell, and LED.

Piezo-phototronic effect in a photodetector

The basic principle of a photon detector is based on the photoelectric effect, in which the

e-h pairs generated by a photon are separated by either a *p-n* junction or a Schottky barrier (Figure 12a). If the Schottky barrier is too high, the holes will be trapped at the semiconductor side so that they cannot be effectively annihilated by the free electrons in the metal (Figure 12a), thus reducing the photocurrent. If the Schottky barrier is too low, the photon-generated electrons cannot be effectively driven away from the interface region, so they can be easily recombined with the holes, which also results in low photocurrent. An optimization of SBH can give the maximum photocurrent. Such a result was observed in a simple photocell.[52]

By tuning the SBH in a ZnO wire-based UV sensor through applying a strain, we can improve the sensitivity of the UV detector, even when the illumination intensity is rather weak.[53] The response of the photodetector is enhanced by 530%, 190%, 9%, and 15% upon 4.1 pW, 120.0 pW, 4.1 nW, and 180.4 nW UV light illumination, respectively, onto the wire by introducing a –0.36% compressive strain in the wire (Figure 12b); this effectively tunes the SBH at the contact by the local piezopotential produced. The sensitivity for weak light illumination is especially enhanced by introducing strain, although the strain has little effect on the sensitivity to stronger light illumination. Our results show that the piezo-phototronic effect can enhance the detection sensitivity more than fivefold

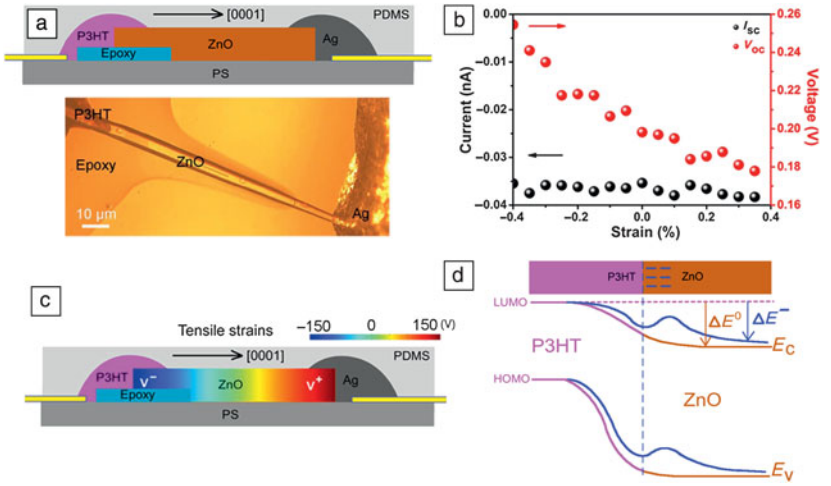

Figure 13. Piezo-phototronic effect in a solar cell. (a) Schematic of a fabricated [0001] type device and top-down optical image of a device. (b) Dependence of short-circuit current I_{sc} and the open-circuit voltage V_{oc} on applied strain. (c) The piezopotential distributions in the stretched device of [0001] type, and the corresponding (d) band diagram of P3HT/ZnO with the presence of negative piezoelectric charges. The blue line indicates the energy band diagram modified by the piezoelectric potential in ZnO.[55]

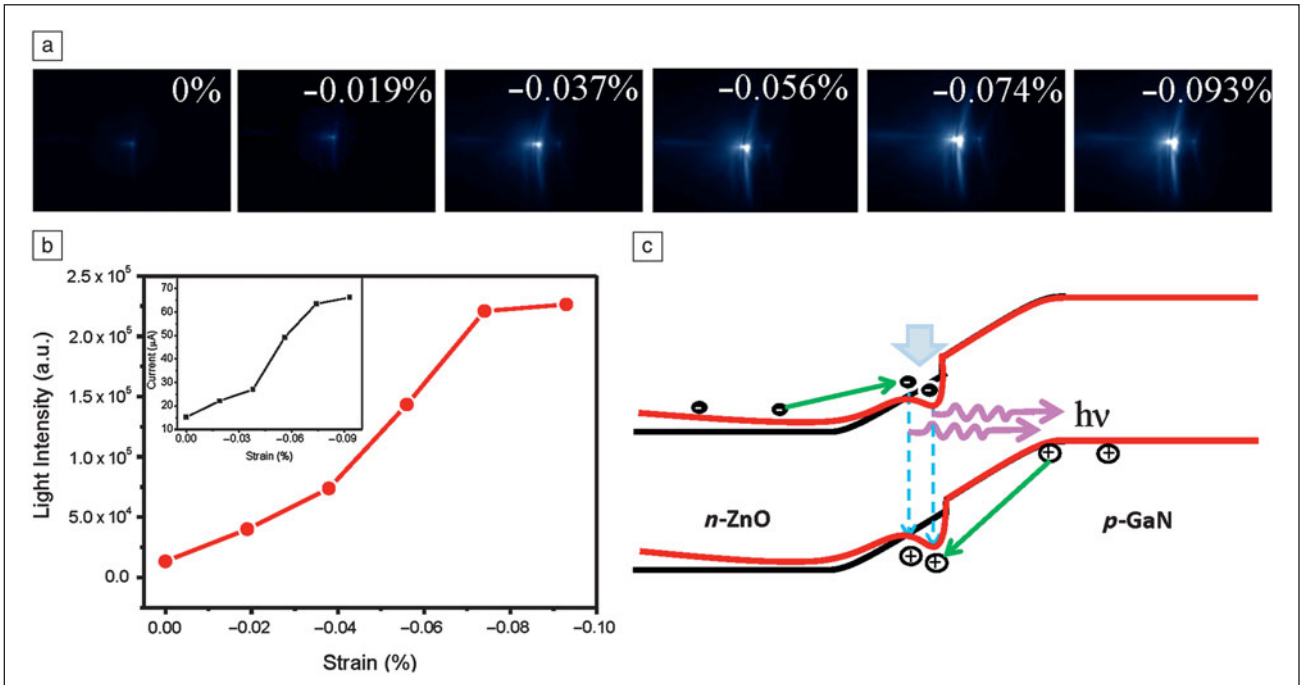

Figure 14. Piezo-phototronic in a GaN/ZnO LED. Enhancement of emission light intensity and conversion efficiency of a (*n*-ZnO wire)-(*p*-GaN film) LED under applied strain. (a) CCD images recorded from the emitting end of a packaged single wire LED under different applied strains. (b) Integrated emission light intensities from the data shown in (a), showing a huge increase in the emission intensity with the increase of the applied compressive strain. The inset is the injection current of the LED at 9 V bias voltage with increase in strain. (c) Schematic energy band diagram of the *p-n* junction without (upper) and with (lower, red line) applied compressive strain, where the channel created at the interface inside ZnO is due to the piezopotential created by strain. The slope of the red line in the lower image at the ZnO side represents the driving effect of the piezopotential on the movement of the charge carriers.[50]

for pW levels of light detection. This conclusion also holds for visible light.[54]

Piezo-phototronic effect in a solar cell

A solar cell uses photon-generated charges, in which the charge separation is critical for conversion efficiency. We now describe a solar cell based on ZnO- poly(3-hexylthiophene) (P3HT) as an example to illustrate the piezo-phototronic effect on the output[55] (**Figure 13**a). ZnO micro/nanowires have a wurtzite structure and grow along the [0001] direction. The short-circuit current I_{sc} and V_{oc} under different strains are shown in Figure 13b. V_{oc} increases and decreases with increasing the compressive and tensile strains, respectively. However, I_{sc} shows a relatively constant value of 0.035 nA under the different strains.

To explain the observed phenomenon, we calculated the distribution of piezopotential in a single ZnO wire. When this device is under tensile strain (Figure 13c), the negative piezopotential is in contact with the P3HT. The negative piezoelectric polarization charges at the interface lift the local conduction band level of ZnO, which can result in a decrease of ΔE and V_{oc} (ΔE^-as shown in Figure 13d).

Piezo-phototronic effect in an LED

Effective charge recombination is essential for an LED. The piezo-phototronic effect can be used to enhance LED output.[34] Our experiments were carried using a *n*-ZnO/*p*-GaN device. A normal force was applied perpendicular to the *p*-*n* junction interface, which produces a tensile strain along the *c*-axis in the ZnO microwire. At a fixed applied bias above the turn-on voltage (3 V), the current and light emission intensity increased with increasing compressive strain (**Figures 14**a–b). The injection current and output light intensity were enhanced by a factor of 4 and 17, respectively, after applying a 0.093% *a*-axis compressive strain, indicating that the conversion efficiency was improved by a factor of 4.25 compared to applying no strain. This means that the external true efficiency of the LED can reach ~7.82% after applying a strain.

The enhanced LED efficiency is due to the piezo-phototronic effect.[6,7] Under an assumption of no-doping or low-doping in ZnO for simplicity, the numerically calculated piezopotential distribution in the ZnO microwire shows (Figure 14c) that a negative potential drop is created along its length when the ZnO microwire is under *a*-axis compressive strain. The finite doping in the wire may partially screen the piezoelectric charges, but it cannot totally eliminate the piezoelectric potential if the doping level is low, thus a dip in the band is possible. The depletion width and internal field decrease under this additional component of forward biased voltage. Subsequently, the injection current and emitting light intensity under the same externally applied forward voltage increase when the device is strained.

Theory of piezo-phototronics

We have developed the theoretical frame of piezo-phototronics by studying photon emission at the *p*-*n* junction and the photon detector with the presence of local piezoelectric charges.[56,57] The analytical results under simplified conditions were derived for understanding the core physics of the piezo-phototronics devices, and the numerical model was developed for illustrating the photon emission process and carriers transport characteristics of the piezoelectric LED in a practical case. Furthermore, the theory for the piezo-phototronic effect on solar cell output has also been developed.[58]

Summary and future perspectives

We have devoted over 12 years to studying ZnO nanostructures. Our systematic studies in the field can be summarized using the analogy of a tree structure, as shown in **Figures 15**. The fundamental "root" of all the science and technologies developed is twofold: (1) the fundamental physics is the piezopotential generated in the inner crystal and the semiconductor properties of the materials themselves; (2) the basic materials systems

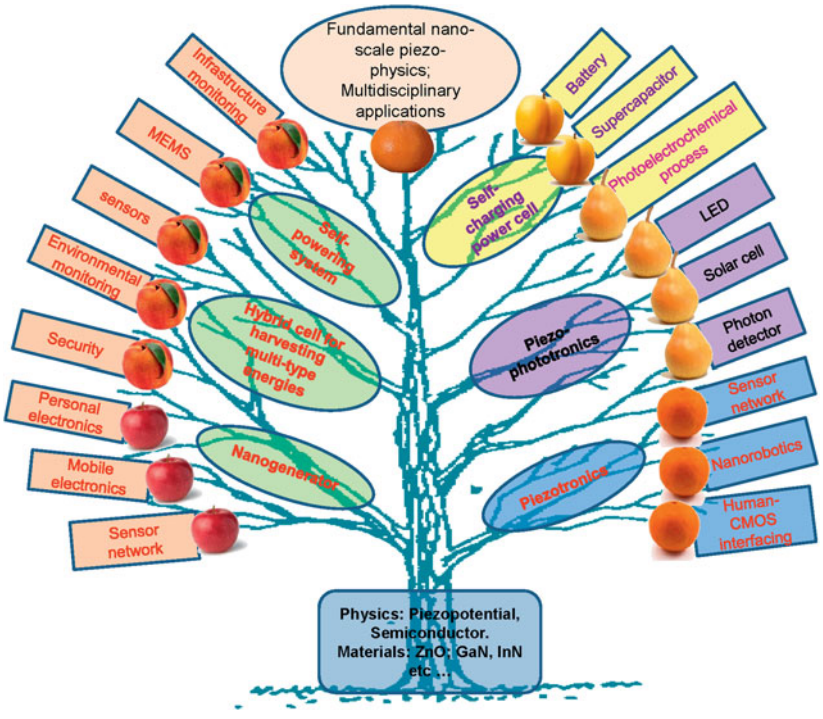

Figure 15. A "tree" representing the fields of nanogenerators, hybrid cells for harvesting multiple types of energies,[36,38,39,60] self-powered systems, piezotronics, piezo-phototronics, and possibly piezophotonics that have been developed by our group in the last decade. The fundamental "root" of all these fields is piezopotential and semiconductor as the basic physics, and ZnO as the fundamental materials system. All of the fields (branches) are derived from these roots.[10]

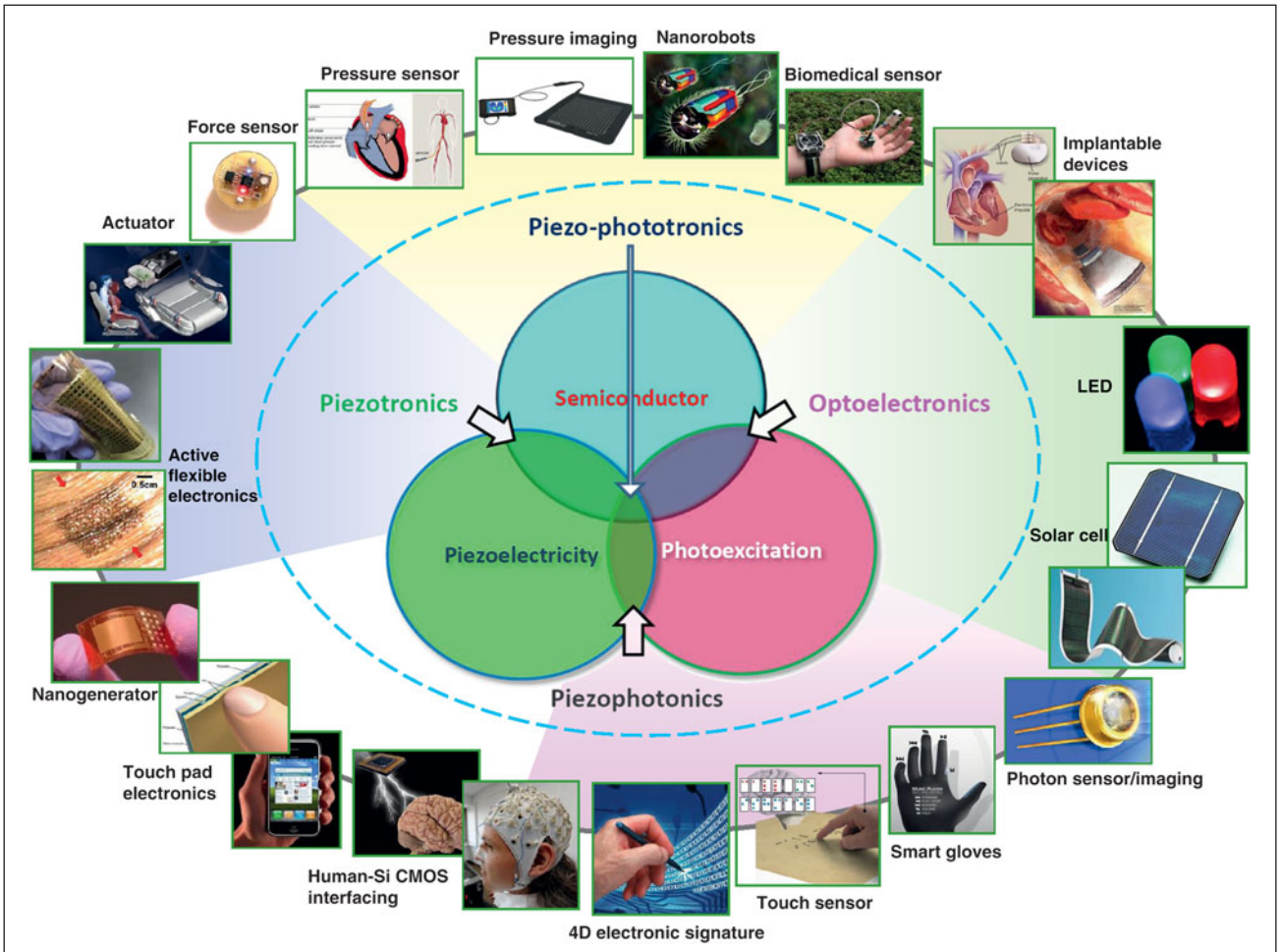

Figure 16. Schematic diagram showing the three-way coupling among piezoelectricity, photoexcitation, and a semiconductor, which is the basis of piezotronics (piezoelectricity-semiconductor coupling), piezophotonics (piezoelectric-photoexcitation coupling), optoelectronics, and piezo-phototronics (piezoelectricity-semiconductor-photoexcitation). Potential applications of piezotronics and piezo-phototronics and nanogenerators are projected, which are important future directions for research and applications.[10]

are wurtzite structures, such as ZnO and GaN. The "branches" are the fields we have developed in the last decade; and the "fruits" are the important near future applications. Furthermore, fundamental physics can be developed by introducing a strain-tuned charge at the interface, and it is possible to study nanoscale piezo-physics and related concepts, which remain to be investigated.

Developing self-powered nanodevices and nanosystems is a step toward going beyond Moore's law. The prototype technology established by the nanogenerator (NG) sets a platform for developing self-powered nanotechnology with important applications in implantable *in vivo* biosensors, wireless and remote sensors for environmental monitoring and infrastructure monitoring, nanorobotics, microelectromechanical systems (MEMS), and personal electronics. We have devoted seven years to developing the NG. For one layer of ZnO nanowires (NWs), the output voltage has now reached 50 V, a current of 120 uA (area size 3 × 3 cm^2), and an ideal peak power of ~0.5 W/cm^3. The near-term goal for NG is to continuously improve the power output and integration with other technology for practical applications.

Energy generation and energy storage are two distinct processes that are usually accomplished using two separated units designed based on different physical principles, such as a piezoelectric nanogenerator and a Li-ion battery; the former converts mechanical energy into electricity, and the latter stores electric energy as chemical energy. Recently, we introduced a method that directly hybridizes the two processes into one, using the mechanical energy that is directly converted and simultaneously stored as chemical energy without going through the intermediate step of first converting it into electricity.[61] By replacing the polyethylene separator, as in a conventional Li battery with a piezoelectric PVDF film, the piezoelectric potential from the PVDF film, as created by mechanical straining, acts as a charge pump to drive Li ions to migrate from the cathode to the anode accompanied by charging reactions at electrodes. This new approach can be applied to fabricate a self-charging power cell for sustainable driving of micro/nano-systems and personal electronics.

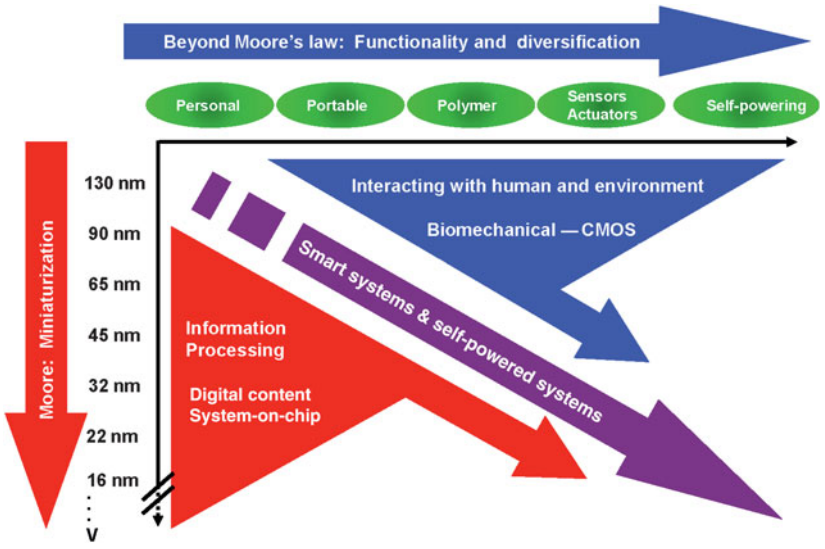

Figure 17. Future of electronics beyond Moore's law. The vertical axis represents a miniaturization and increase of device density, CPU speed, and memory. The horizontal axis represents the diversity and functionality of personal and portable electronics.[10]

Moore's law has been the roadmap that directs and drives information technology in the last few decades (see the vertical axis in **Figure 17**). Sensor networks and personal health care have been predicted as major driving forces for industry in the near-term future. As we have observed in today's electronic products, electronics are moving toward personal electronics, portable electronics, and polymer-based flexible electronics. We are looking for multifunctionality and diversity associated with electronics. The drive for technology in the last half century is miniaturization and portability/mobility. For example, having a super-fast computer in a mobile phone may not be the major driver for future markets, but consumers are looking for more functionality, such as healthcare sensors for blood pressure, body temperature, and blood sugar level, and interfacing with the environment using sensors for detecting gases, UV, and hazardous chemicals. In such a case, IT is developing along another dimension, as presented in the horizontal axis in Figure 17. The near future development of electronics is moving toward integrating electronics with multifunctional sensors and self-powered technology. The goal is to directly interface humans with the environment in which we live in. A combination of CPU speed, density of memory and logic, along with functionality, tends to drive electronics toward smart systems and self-powered systems, which are believed to be the direction for near-term electronics.

Piezotronics uses piezopotential as the gate voltage for tuning the charge carrier transport processes at an M-S contact or *p-n* junction. The design of piezotronics may fundamentally change the design of traditional field-effect transistors by eliminating the gate electrode, replacing the externally applied gate voltage with an internally created piezopotential, and controlling the transport of charges through the contact at the drain (source)-NW interface rather than the channel width. Piezotronics can be used with silicon-based complementary metal oxide semiconductor (CMOS) technology, because it can be integrated on a polymer substrate for fabricating active, flexible electronics. Silicon technology provides the speeds and density of devices, while piezotronics provides the functionality required for human-CMOS interfacing. Piezotronics has the potential to serve as a mechanosensation in physiology,[59] which is about the mechanical stimulations of senses (touch, hearing and balance, and pain), to convert mechanical stimuli into neuronal signals; the former is a mechanical actuation, and the latter is electrical stimulation. Piezotronics has potential applications in human-Si technology interfacing, smart MEMS, nanorobotics, and sensors (**Figure 16**).

Piezo-phototronics is a result of a three-way coupling among piezoelectricity, photonic excitation, and semiconductor transport, which allows for the tuning and controlling of carrier generation, separation, transport, and/or a recombination of charge carriers in optoelectronic processes by strain-generated piezopotential. The development of this field will have great impact on LEDs, photodetectors and solar cells fabricated using wurtzite and other materials (Figure 16).The piezotronics and piezo-phototronics were invented for such purposes, and they are considered to be *active* flexible electronics or bio-driven electronics.

Acknowledgments

This research was supported by DARPA, NSF, BES DOE, NIH, NASA, US Airforce, MANA, NIMS (Japan), Samsung, Chinese Academy of Sciences, and Georgia Tech. Thanks to the contributions made by my group members (not in any particular order): Yong Ding, Puxian Gao, Jinhui Song, Xudong Wang, Rusen Yang, Jun Zhou, Yong Qin, Sheng Xu, Zhengwei Pan, Zurong Dai, Will Hughes, Jin Liu, Yifan Gao, Jr-Hau He, Ming-Pei Lu, Jung-il Hong, Chen Xu, Yaguang Wei, Wenzhuo Wu, Youfan Hu, Yan Zhang, Qing Yang, Weihua Liu, Yifeng Lin, Minbaek Lee, Peng Fei, Ying Liu, Chi-Te Huang, Tei-Yu Wei, Ben Hansen, Caofeng Pan, Guang Zhu, Ya Yang, Ying Liu, Sihong Wang, Yusheng Zhou, Xiaonan Wen, Long Lin, Simiao Niu, Xinyu Xue, Lin Dong, and more; and my collaborators: Charles M. Lieber, L.-J. Chen, S.Y. Lu, L.J. Chou, R.L. Snyder, R. Dupuis, J.F. Wu, Gang Bao, Liming Dai, Jing Zhu, Yue Zhang, Aifang Yu, Peng Jiang, M. Willander, C. Falconi.

References

1. Z.L. Wang, *Mater. Sci. Eng. R* **64**, 33 (2009).
2. Z.L. Wang, J.H. Song, *Science* **312**, 242 (2006).
3. Z.L. Wang, *Adv. Funct. Mater.* **18**, 3553 (2008).

4. Z.L. Wang, R.S. Yang, J. Zhou, Y. Qin, C. Xu, Y.F. Hu, S. Xu, *Mater. Sci. Eng. R* **70**, 320 (2010).
5. Z.L. Wang, *Nanogenerators for Self-Powered Devices and Systems* (Georgia Institute of Technology, SMARTech digital repository, 2011); http://hdl.handle.net/1853/39262.
6. Z.L. Wang, *Nano Today* **5**, 540 (2010).
7. Z.L. Wang, *Adv. Mater.* (2012); doi:10.1002/adma.201104365.
8. Z.W. Pan, Z.R. Dai, Z.L. Wang, *Science* **291**, 1947 (2001).
9. Z.L. Wang, *Mater. Today* **7**, 26 (2004).
10. Z.L. Wang, X.Y. Kong, Y. Ding, P.X. Gao, W. Hughes, R.S. Yang, Y. Zhang, *Adv. Funct. Mater.* **14**, 944 (2004).
11. X.Y. Kong, Z.L. Wang, *Nano Lett.* **3**, 1625 (2003).
12. X.Y. Kong, Y. Ding, R.S. Yang, Z.L. Wang, *Science* **303**, 1348 (2004).
13. W.L. Hughes, Z.L. Wang, *J. Am. Chem. Soc.* **126**, 6703 (2004).
14. P.X. Gao, Y. Ding, W.J. Mai, W.L. Hughes, C.S. Lao, Z.L. Wang, *Science* **309**, 1700 (2005).
15. M. Law, L.E. Greene, J.C. Johnson, R. Saykally, P.D. Yang, *Nat. Mater.* **4**, 455 (2005).
16. X.D. Wang, J. Zhou, C.S. Lao, J.H. Song, N.S. Xu, Z.L. Wang, *Adv. Mater.* **19**, 1627 (2007).
17. M.H. Huang, S. Mao, H. Feick, H.Q. Yan, Y.Y. Wu, H. Kind, E. Weber, R. Russo, P.D. Yang, *Science* **292**, 1897 (2001).
18. J.H. Lim, C.K. Kang, K.K. Kim, I.K. Park, D.K. Hwang, S.J. Park, *Adv. Mater.* **18**, 2720 (2006).
19. X.D. Wang, J.H. Song, J. Liu, Z.L. Wang, *Science* **316**, 102 (2007).
20. Y. Qin, X.D. Wang, Z.L. Wang, *Nature* **451**, 809 (2008).
21. Q.X. Zhao, M. Willander, R.R. Morjan, Q.H. Hu, E.E.B. Campbell, *Appl. Phys. Lett.* **83**, 165 (2003).
22. X.D. Wang, C.J. Summers, Z.L. Wang, *Nano Lett.* **3**, 423 (2004).
23. S. Xu, Z.L. Wang, *Nano Res.* **4**, 1013 (2011).
24. Y.G. Wei, W.Z. Wu, R. Guo, D.J. Yuan, S. Das, Z.L. Wang, *Nano Lett.* **10**, 3414 (2010).
25. S. Xu, C.S. Lao, B. Weintraub, Z.L. Wang, *J. Mater. Res.* **23**, 2072 (2008).
26. Z.L. Wang, *Sci. Am.* **298**, 82 (2008).
27. Y.F. Hu, L. Lin, Y. Zhang, Z.L. Wang, *Adv. Mater.* **24**, 110 (2012).
28. R.S. Yang, Y. Qin, L.M. Dai, Z.L. Wang, *Nat. Nanotechnol.* **4**, 34 (2009).
29. G. Zhu, R.S. Yang, S.H. Wang, Z.L. Wang, *Nano Lett.* **10**, 3151 (2010).
30. Y.F. Hu, L. Lin, Y. Zhang, Z.L. Wang, *Adv. Mater.* **24**, 110 (2012).
31. Y.F. Hu, Y. Zhang, C. Xu, G. Zhu, Z.L. Wang, *Nano Lett.* **10**, 5025 (2010).
32. J.H. Jung, M.B. Lee, J.-I. Hong, Y. Ding, C.-Y. Chen, L.-J. Chou, Z.L. Wang, *ACS Nano* **5**, 10041 (2011).
33. S. Xu, Y. Qin, C. Xu, Y.G. Wei, R.S. Yang, Z.L. Wang, *Nat. Nanotechnol.* **5**, 366 (2010).
34. Y.F. Hu, Y. Zhang, C. Xu, L. Lin, R.L. Snyder, Z.L. Wang, *Nano Lett.* **11**, 2572 (2011).
35. M.B. Lee, J.H. Bae, J.Y. Lee, C.S. Lee, S.H. Hong, Z.L. Wang, *Energy Environ. Sci.* **4**, 3359 (2011).
36. C. Xu, X.D. Wang, Z.L. Wang, *J. Am. Chem. Soc.* **131**, 5866 (2009).
37. C. Xu, Z.L. Wang, *Adv. Mater.* **23**, 873 (2011).
38. B.J. Hansen, Y. Liu, R.S. Yang, Z.L. Wang, *ACS Nano* **4**, 3647 (2010).
39. C.F. Pan, Z.T. Li, W.X. Guo, J. Zhu, Z.L. Wang, *Angew. Chem. Int. Ed.* **50**, 11192 (2011).
40. A.F. Yu, P. Jiang, Z.L. Wang, *Nano Energy* (2012); doi:10.1016/j.nanoen.2011.12.006.
41. Y. Zhang, Y. Liu, Z.L. Wang, *Adv. Mater.* **23**, 3004 (2011).
42. X.D. Wang, J. Zhou, J.H. Song, J. Liu, N.S. Xu, Z.L. Wang, *Nano Lett.* **6**, 2768 (2006).
43. J.H. He, C.L. Hsin, J. Liu, L.J. Chen, Z.L. Wang, *Adv. Mater.* **19**, 781 (2007).
44. Z.L. Wang, *Adv. Mater.* **19**, 889 (2007).
45. P.W. Bridgman, *Phys. Rev.* **42**, 858 (1932).
46. C.S. Smith, *Phys. Rev.* **94**, 42 (1954).
47. J. Zhou, P. Fei, Y.D. Gu, W.J. Mai, Y.F. Gao, R.S. Yang, G. Bao, Z.L. Wang, *Nano Lett.* **8**, 3973 (2008).
48. Q. Yang, W.H. Wang, S. Xu, Z.L. Wang, *Nano Lett.* **11**, 4012 (2011).
49. W.Z. Wu, Y.G. Wei, Z.L. Wang, *Adv. Mater.* **22**, 4711 (2010).
50. W.Z. Wu, Z.L. Wang, *Nano Lett.* **11**, 2779 (2011).
51. Y.F. Hu, Y.L. Chang, P. Fei, R.L. Snyder, Z.L. Wang, *ACS Nano* **4**, 1234 (2010).
52. Y.F. Hu, Y. Zhang, Y.L. Chang, R.L. Snyder, Z.L. Wang, *ACS Nano* **4**, 4220 (2010).
53. Q. Yang, X. Guo, W.H. Wang, Y. Zhang, S. Xu, D.H. Lien, Z.L. Wang, *ACS Nano* **4**, 6285 (2010).
54. Y. Liu, Q. Yang, Y. Zhang, Z.Y. Yang, Z.L. Wang, *Adv. Mater.*, in press (2012).
55. Y. Yang, W.X. Guo, Y. Zhang, Y. Ding, X. Wang, Z.L. Wang, *Nano Lett.* **11**, 4812 (2011).
56. Y. Liu, Q. Yang, Y. Zhang, Z.Y. Yang, Z.L. Wang, *Adv. Mater.* **24**, 1410 (2012).
57. Y. Zhang, Z.L. Wang, *Adv. Mater.*, in press (2012).
58. Y. Zhang, Y. Yang, Z.L. Wang, *Energy Environ. Sci.* **5**, 6850 (2012).
59. http://en.wikipedia.org/wiki/Mechanosensation.
60. D. Choi, M.J. Jin, K.Y. Lee, S.-G. Ihn, S. Yun, X. Bulliard, W. Choi, S.Y. Lee, S.-W. Kim, J.-Y. Choi, J.M. Kim, Z.L. Wang, *Energy Environ. Sci.* **4**, 4607 (2011).
61. X.Y. Xue, S.H. Wang, W.X. Guo, Y. Zhang, Z.L. Wang, *Nano Lett.*; doi: 10.1021/n13028791 (2012). □

Zhong Lin Wang is the Hightower Chair in materials science and engineering, a Regents' Professor, and an Engineering Distinguished Professor and director of the Center for Nanostructure Characterization at the Georgia Institute of Technology. He received his PhD degree from Arizona State University in 1987. He was elected as a foreign member of the Chinese Academy of Sciences in 2009; a member of the European Academy of Sciences in 2002; and Fellow of the American Physical Society in 2005, of AAAS in 2006, of the Materials Research Society in 2008, of the Microscopy Society of America in 2010, and of the World Innovation Foundation in 2002. He received the 2012 Edward Orton Memorial Lecture Award from the American Ceramic Society, the 2011 MRS Medal from the Materials Research Society, the 1999 Burton Medal from the Microscopy Society of America, the 2001 S.T. Li prize for Outstanding Contribution in Nanoscience and Nanotechnology, the 2009 Purdy Award from the American Ceramic Society, and the NanoTech Briefs Top 50 award in 2005. Wang has authored and co-authored five scientific reference books and textbooks and more than 730 peer-reviewed journal articles, 50 review papers, and book chapters. He also holds 32 patents. Wang can be reached by email at Zhong.wang@mse.gatech.edu.